Thermal and Light Control of the Sol-Gel Phase Transition in Cholesterol-Based Organic Gels. Novel Helical Aggregation Modes As Detected by Circular Dichroism and Electron Microscopic Observation

Kazutaka Murata, Masayoshi Aoki, Tsuyoshi Suzuki, Takaaki Harada, Hirosuke Kawabata, Takashi Komori, Fumio Ohseto, Keiko Ueda, and Seiji Shinkai*

Contribution from the Chemirecognics Project, ERATO, Research Development Corporation of Japan, Aikawa 2432-3, Kurume, Fukuoka 830, Japan

Received November 15, 1993. Revised Manuscript Received May 2, 1994®

Abstract: Nineteen cholesterol derivatives containing a variety of azobenzene moieties coupled to C-3 of a steroidal moiety through an ester linkage were synthesized. We employed two different esterification methods by which cholesterol derivatives with the natural (*S*)-configuration at C-3 and those with the inverted (*R*)-configuration at C-3 were obtained (the latter derivatives are indicated by a prime). Among them, cholesterol derivatives bearing a *p*-alkoxyazobenzene moiety (**2R** and **2R'**) acted as excellent thermally-reversible gelators of various organic fluids, but the gelation ability is fairly different between **2R** and **2R'**: **2R** could gelatinize hydrocarbons such as *n*-hexane, *n*-octane, and toluene, halogen solvents such as 1,2-dichloroethane and dichloromethane, ether solvents such as diethyl ether and THF, and alcohols such as ethanol and 1-butanol whereas **2R'** could gelatinize ketones, methanol, and polysiloxanes. In general, the solubility of **2R'** in apolar solvents is superior to that of **2R**, so **2R** is useful for gelation of apolar solvents whereas **2R'** is useful for gelation of polar solvents. We found that the sol-gel phase transition is sensitively "read-out" by a change in the circular dichroism (CD) spectrum: the gel phase is CD-active whereas the sol phase is totally CD-silent. For example, the **2Me**-1-butanol gel gave a positive exciton coupling band with (*R*)-chirality whereas the **2Et'**-methanol gel gave a negative exciton coupling band with (*S*)-chirality. These results mean that dipoles in the azobenzene moiety are oriented in a clockwise (in (*R*)-chirality) or anticlockwise (in (*S*)-chirality) direction when they interact in the excited state. Strangely, we accidentally found that *the CD sign of the gels prepared from* ***2Pr', 2Bu, and 3Me'*** *(azobenzene-linked cholesterol derivative with p-NMe_2) is frequently inverted.* After careful examination of the gel preparation conditions, we found that inversion takes place only when the cooling speed is fast. The scanning electron microscopic studies established that gelators form three-dimensional networks with helical fibrils. Interestingly, we found that in the **3Me'** gel prepared from cyclohexane *the gel with (R)-chirality in CD possesses a right-handed helix whereas the gel with (S)-chirality in the CD possesses a left-handed helix.* The sol-gel phase transition was also induced by photoresponsive *cis-trans* isomerism of the azobenzene moiety: the gel formed from the *trans*-isomer was efficiently converted to the sol when *trans*-to-*cis* isomerization was photochemically induced, and this process can be repeated reversibly. The photoinduced sol-gel phase transition was also "read-out" as a change in CD spectroscopy.

Introduction

Cholesterols are versatile building blocks which support not only the architectures observed in biological systems but also the formation of liquid crystals,[1-5] bilayer membranes,[6,7] monolayers at the air-water interface,[8] etc., in artificial systems. These properties are basically related to the molecular rigidity, aggregative nature, asymmetric carbons, etc., which are all characteristics of the cholesterol skeleton. Recently, Lin et al.[9-11] found a new family of gelators for organic fluids which contain a 2-substituted anthracenyl-type group coupled to C-3 of a steroidal moiety. The finding indicates that the aggregative nature of the cholesterol skeleton, which usually tends to form liquid-crystalline aggregates, is also operative in the gelation of organic fluids. Several (but not many) low-molecular-weight gelators without the cholesterol skeleton were also reported: they have a hydrogen-bonding donor-and-acceptor couple or a charged plus-and-minus couple within a molecule which is essential to molecular aggregation in solution.[12] In contrast, in the cholesterol-based gelators, the driving force for molecular aggregation should be relatively weak interactions such as a dipole-dipole interaction and a van der Waals interaction. Aiming for the development of more efficient cholesterol-based gelators, we previously synthesized cholesterol derivatives containing an azobenzene group with a large dipole moment at C-3 of a steroidal skeleton.[13] Surprisingly, some of them served as "supergelators" which can gelatinize various organic solvents with less than 1 wt % of the cholesterol derivatives.[12] We thus considered that this system would merit further investigation.

* Abstract published in *Advance ACS Abstracts*, June 15, 1994.

(1) For a recent review, see: Weiss, R. G. *Tetrahedron* **1988**, *44*, 3413.
(2) Eskenazi, C.; Nicond, J. F.; Kagan, H. B. *J. Org. Chem.* **1979**, *44*, 995.
(3) Leigh, W. J.; Mitchell, D. S. *J. Am. Chem. Soc.* **1988**, *110*, 1311.
(4) Anderson, V. C.; Craig, B. B.; Weiss, R. G. *J. Am. Chem. Soc.* **1982**, *104*, 2972.
(5) He, G.-X.; Wada, F.; Kikukawa, K.; Shinkai, S.; Matsuda, T. *J. Org. Chem.* **1990**, *55*, 541 and reference cited therein.
(6) Echegoyen, L. E.; Portugal, L.; Miller, S. R.; Hernandez, J. C.; Echegoyen, L.; Gokel, G. W. *Tetrahedron Lett.* **1988**, *29*, 4065.
(7) Fasoli, H.; Echegalyen, L. E.; Hernandez, J. C.; Gokel, G. W.; Echegoyen, L. *J. Chem. Soc., Chem. Commun.* **1989**, 578.
(8) Nishi, T.; Shinkai, S. *Chem. Express* **1993**, *8*, 173.
(9) Lin, Y.-C.; Weiss, R. G. *Macromolecules* **1987**, *20*, 414.
(10) Lin, Y.-C.; Kachar, B.; Weiss, R. G. *J. Am. Chem. Soc.* **1989**, *111*, 5542.
(11) Furman, I.; Weiss, R. G. *Langmuir* **1993**, *9*, 2084.
(12) For gelators without a cholesterol skeleton, see: (a) Brotin, T.; Utermolhlen, R.; Fages, F.; Bouas-Laurent, H.; Desvergne, J. P. *J. Chem. Soc., Chem. Commun.* **1991**, 416. (b) Twieg, R. J.; Russell, T. P.; Siemens, R.; Robolt, J. F. *Macromolecules* **1985**, *18*, 1361. (c) Aoki, M.; Murata, K.; Shinkai, S. *Chem. Lett.* **1991**, 1715. (d) Aoki, M.; Nakashima, K.; Kawabata, H.; Tsutsui, S.; Shinkai, S. *J. Chem. Soc., Perkin Trans. 2* **1993**, 347. (e) Hanabusa, K.; Okui, K.; Karaki, K.; Koyama, T.; Shirai, H. *J. Chem. Soc., Chem. Commun.* **1992**, 1371 and references cited therein. Cholesterol-based gelators were also studied by Terech et al.: (a) Wade, R. H.; Terech, P.; Hewat, E. A.; Ramasseul, R.; Volino, F. *J. Colloid Interface Sci.* **1986**, *114*, 442. (b) Terech, P. *ibid.* **1985**, *107*, 244. Terech, P. *Liq. Cryst.* **1991**, *9*, 59.
(13) Murata, K.; Aoki, M.; Nishi, T.; Ikeda, A.; Shinkai, S. *J. Chem. Soc., Chem. Commun.* **1991**, 1715.

0002-7863/94/1516-6664$04.50/0

Here, it occurred to us that (i) if the gel formation is supported by the stacking of *trans*-azobenzenes covalently linked to the "*chiral*" cholesterol, the aggregation should occur in an asymmetric manner and the sol–gel phase transition should be "*read-out*" as a change in circular dichroism (CD), (ii) the sol–gel phase transition should be reversibly controlled by *trans–cis* photoisomerization in the azobenzene moiety, and (iii) the sol–gel phase transition temperature should be affected by the steric and electrostatic effects which are brought about by the structural change in the azobenzene moiety. With these objects in mind we fully characterized azobenzene-appended cholesterol-based gelators. We have found a number of novel gelation behaviors, that is, (i) solvent effects, (ii) substitutent effects in the azobenzene moiety, (iii) effects of the absolute configration at C-3, (iv) photoresponsiveness, (v) competition of right-handed versus left-handed helixes in the gel network,[14] (vi) inversion of chirality, and (vii) observation of the helically-developed, fibrous aggregates with an electron microscope. These findings are all ascribed to a unique character of cholesterol-based gelators; that is, they can form one-dimensional, helical aggregates in solution.

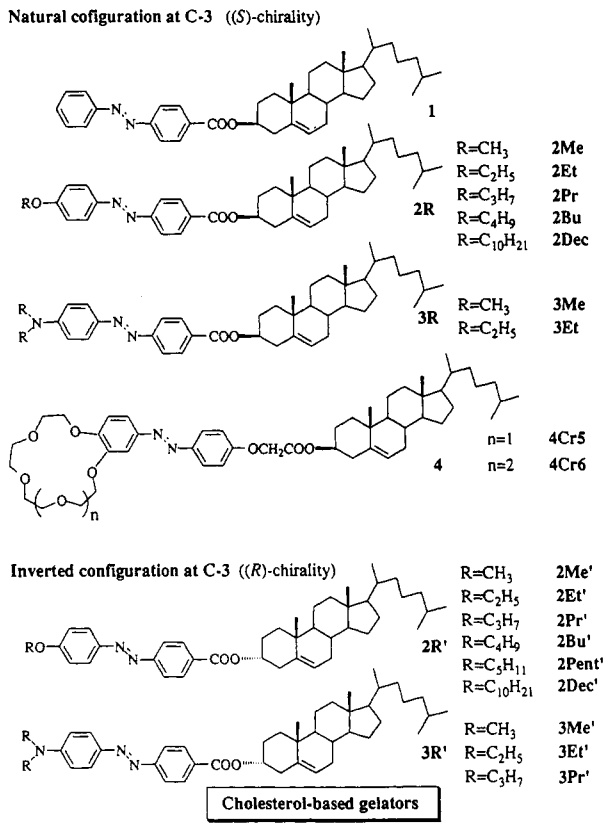

Results and Discussion

Effects of Solvents, Substituents, and C-3 Configuration on Gel Stability. When cholesterol esters are synthesized by the reaction of cholesterol and acid chlorides, the absolute configuration at C-3 is retained as the natural configuration (*i.e.*, (*S*)-chirality: (eq 1)). Table 1 shows the results of the gelation tests for **1**, **2R**, **3R**, and **4** with (*S*)-chirality. It can be seen from Table 1 that azobenzene-linked cholesterol derivatives act as gelators of various organic fluids. In particular, **2R**-type compounds act as excellent gelators of hydrocarbon solvents such as *n*-hexane, *n*-octane, and toluene, halogen solvents such as 1,2-dichloroethane and dichloromethane, ether solvents such as diethyl ester and THF, and alcohols such as ethanol, 1-butanol, and 1-octanol. It is really surprising that in some cases the gelation is observed even in the presence of less than 1 wt % gelator (classified as "supergelators" (SG) in Table 1) and even acetic acid, amines, and polysiloxanes

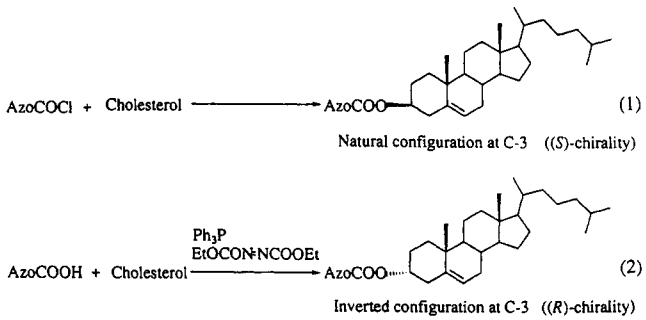

are gelatinized. The gelation ability of **3R**-type compounds is generally inferior to that of **2R**-type compounds. Compound **4Cr6** with a benzo-18-crown-6 moiety acts as a gelator of several hydrocarbons and alcohols whereas compound **4Cr5** with a benzo-15-crown-5 moiety is easily recrystallized from various solvents and does not give a stable organic gel. From dioxane and methyl ethyl ketone, **2Me** and **2Pr** gave gels whereas **2Et** and **2Bu** are recrystallized. The results suggest that the "odd–even effect" in the R group may be operative in gel formation.

When cholesterol and carboxylic acids are treated with triphenylphosphine and diethyl azenedicarboxylate, inversion of C-3 takes place (i.e., (*R*)-chirality (eq 2)).[15] Interestingly, the gelation ability of these cholesterol derivatives with (*R*)-chirality (expressed by a prime, Table 2) is remarkably different from that of cholesterol derivatives with (*S*)-chirality. For example, **2R'** could not gelatinize aromatic hydrocarbons, halogen solvents, and carbon disulfide, which were gelatinized by **2R**. In contrast, the gelation ability toward ketones, methanol, and polysiloxanes was markedly enhanced. The "odd–even effect" in the R group is also seen for **2R'**: for example, diethyl ether was gelatinized by **2Et'** and **2Bu'** but not by **2Me'** and **2Pr'**. In general, cholesterol derivatives of a **2R'** series showed a gelation ability higher than that of a **2R** series. The gelation ability increased with an increase in the R length, and in particular, **2Dec'** with a decyl group could gelatinize most of the organic solvents tested herein. The gels prepared from **2R** were turbid in some cases whereas those prepared from **2R'** were highly transparent. The propanol and butanol gels of **2Bu'** were stable for more than 2 years. It is also worthy to mention that there are many I (insoluble) marks in Table 1 whereas such marks are seen only for methanol, glycerol, and water in Table 2. In a **3R'** series only **3Me'** showed a significant gelation ability. **3Et'** and **3Pr'** are more soluble in most organic solvents than **3Me'**, and therefore, their gelation ability was generally poorer.

From the foregoing gelation tests, it was found that, in general, **2R** derivatives with naturally-occurring (*S*)-chirality feature low solubility, high cohesive forces, and high crystallinity whereas **2R'** derivatives with inverted (*R*)-chirality feature high solubility, low cohesive forces, and low crystallinity. This is also true in the solid phase: in general, the **2R** derivatives have mp's higher than those of the corresponding **2R'** derivatives (see the Experimental Section). The "gel phase" appears on the border of the solution phase and the solid phase, so that gelators are required to possess both moderate affinity with solvent molecules and the moderate self-aggregation ability. Comparision of Table 1 with Table 2 reveals that these two factors are well balanced in **2R** and **2R'** derivatives: **2R** derivatives having low solubility have a tendency to gelatinize "good" solvents whereas **2R'** derivatives having high solubility have a tendency to gelatinize "poor" solvents. For example, **2R'** derivatives are too soluble in aromatic hydrocarbons, halogen solvents, and ethers to gelatinize them, but the less soluble **2R** derivatives can gelatinize them. **2R** derivatives are almost insoluble in methanol and acetonitrile, but **2R'** derivatives are moderately soluble in these solvents and gelatinize them.

Figure 1 shows energy-minimized structures of **2Me** and **2Me'**. It is seen from Figure 1 that **2Me** with the natural (*S*)-

(14) Preliminary communication: Murata, K.; Aoki, M.; Shinkai, S. *Chem. Lett.* **1992**, 739.

(15) Bose, A.; Lal, B.; Hoffman, W. A.; Manhas, M. S. *Tetrahedron Lett.* **1973**, *18*, 1119.

Table 1. Gelation Ability of Cholesterol-Based Gelators **1**, **2R**, **3R**, and **4** with (*S*)-Chirality[a]

		2R					3R		4	
solvent	1 R = H	2Me (R = MeO)	2Et (R = EtO)	2Pr (R = Pr^nO)	2Bu (R = Bu^nO)	2Dec (R = Dec^nO)	3Me (R = Me_2N)	3Et (R = Et_2N)	4Cr5 (R = B15Cr5)	4Cr6 (R = B18Cr6)
n-hexane	R	SGc	SGc	Gc	R	R	R	R	R	Gf′
n-octane	Gc	SGc	SGc	Gc	Gc	R	R	R	R	G
paraffin	S	Gf	G	G	G	G	G	G	S	Gf
cyclohexane	R	Gc	R	R	R	R	R	S	R	G
decalin	S	G	Gc	Gc	Gc	Gc	R	Gc	R	Gf′
carbon tetrachloride	S	S	R	R	R	Gs	R	R	R	S
carbon disulfide	Gf	Gf	Gs	Gs	Gs	Gs	R	S	S	Gf
benzene	S	S	S	S	S	S	S	S	S	S
toluene	Gc	Gc	Gc	Gc	Gc	G	Gc	S	R	S
nitrobenzene	G	G	G	G	G	G	R	G	S	G
1,2-dichloroethane	G	G	Gc	Gc	Gc	G	Gc	S	S	S
dichloromethane	S	S	Gc	Gc	Gs	Gc	Gc	S	S	S
chloroform	S	S	S	S	S	S	S	S	S	S
diethyl ether	Gs	Gs	SGc	Gc	R	R	R	R	I	S
tetrahydrofuran	R	Gf′	Gs	Gs	Gs	Gs	Gs	S	S	S
1,4-dioxane	Gc	Gc	R	Gc	R	G	R	R	S	S
ethyl acetate	R	SGc	R	R	R	R	R	R	S	S
acetone	R	SGc	R	R	R	R	R	R	S	R
methyl ethyl ketone	R	G	R	Gc	R	R	R	R	S	S
N,*N*-dimethylformamide	R	G	Gc	Gc	Gc	Gc	R	R	S	Gf′
dimethyl sulfoxide	SGc	G	Gc	SG	SG	SGc	R	R	S	G
acetonitrile	I	I	I	I	I	I	I	I	S	R
methanol	I	I	I	I	I	I	I	I	S	I
ethanol	I	SGc	R	SGc	SGc	R	R	R	S	Gf′
1-butanol	R	SGc	R	SGc	SGc	R	R	R	S	G
1-octanol	R	G	G	G	G	Gc	Gc	Gs	S	G
acetic acid	R	SGc	SGc	SGc	SGc	R	R	I	S	G
propylamine	Gc	Gc	R	Gc	Gc	R	R	R	S	S
diethylamine	Gc	Gc	Gc	Gc	Gc	R	I	R	S	S
aniline	S	G	G	G	G	G	Gs	S	S	Gs
pyridine		G	G	G	G	G	S	S	S	S
dimethylpolysiloxane (1cs)	R	SG	R	R	R	R	R	R	S	G
dimethylpolysiloxane (6cs)	R	SG	I	I	I	I	I	I	S	G
glycerol	I	I	I	I	I	I	I	I	I	I
water	I	I	I	I	I	I	I	I	I	I

[a] [Gelator] = 1–7 wt %; G = gel formed when cooled at 2–20 °C and stable at room temperature (*ca.* 20–25 °C), Gs = gel formed but turned into solution at room temperature, Gc = gel formed but turned into crystals at room temperature, SG = supergelator in which gel was formed at [gelator] < 1 wt %, Gf = gel formed when cooled in a refrigerator (at –6 °C) and stable at room temperature, Gf′ = gel formed when cooled in a refrigerator (at –6 °C) but not stable at room temperature; Gel not formed because of crystallization (R), solubilization (S), or insolubilization (I).

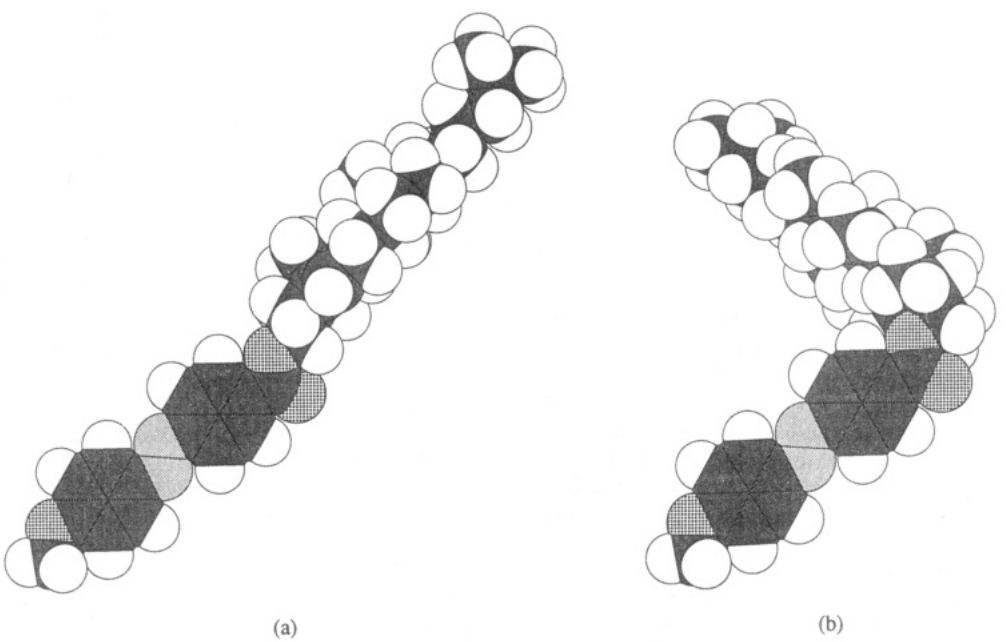

(a) (b)

Figure 1. Energy-minimized structures of (a) **2Me** and (b) **2Me′**.

configuration at C-3 adopts an extended conformation and the dihedral angle between the cholesterol plane and the azobenzene plane is about 90° whereas **2Me′** with the inverted (*R*)-configuration at C-3 adopts an L-shaped bent conformation.

Table 2. Gelation Ability of Cholesterol-Based Gelators **2R′** and **3R′** with (*R*)-Chirality[a]

	2R′						**3R′**		
solvent	**2Me′** (R = MeO)	**2Et′** (R = EtO)	**2Pr′** (R = Pr^nO)	**2Bu′** (R = Bu^nO)	**2Pent′** (R = Pe^nO)	**2Dec′** (R = Dec^nO)	**3Me′** (R = Me_2N)	**3Et′** (R = Et_2N)	**3Pr′** (R = Pr_2^nN)
n-hexane	Gf	G	G	G	G	G	R	Gf′	S
n-heptane	Gf	G	G	G	G	G	R	G	S
n-octane	Gf	G	G	G	G	G	R	S	S
paraffin	G	G	G	G	G	G	Gf	S	S
cyclohexane	S	S	S	S	S	G	SG	S	S
methylcyclohexane	S	Gf	Gf	Gf	G	G	SG	S	S
decalin	S	S	S	Gf′	Gf′	G	G	S	S
carbon tetrachloride	S	S	S	S	S	S	S	S	S
carbon disulfide	S	S	S	S	S	Gf′	Gf	S	S
benzene	S	S	S	S	S	S	S	S	S
toluene	S	S	S	S	S	Gf	R	S	S
p-xylene	S	S	S	S	S	S	Gc	S	S
nitrobenzene	S	S	S	S	S	G	G	S	S
m-cresol	S	S	S	S	S	Gs	S	S	S
1,2-dichloroethane	S	S	S	S	S	Gs	G	S	S
dichloromethane	S	S	S	S	S	S	S	S	S
chloroform	S	S	S	S	S	S	S	S	S
diethyl ether	S	Gs	S	Gs	G	G	Gs	S	S
dipropyl ether	S	Gf′	Gf′	Gf′	Gf′	G	Gs	S	S
diphenyl ether	S	S	S	S	S	G	G	S	S
tetrahydrofuran	S	S	S	S	S	S	S	S	S
1,4-dioxane	S	S	S	S	S	G	Gc	S	S
ethyl formate	Gf	G	G	G	G	G	R	S	S
methyl acetate	S	G	G	G	G	G	SGc	S	S
ethyl acetate	S	Gf	Gf	Gf	G	G	Gf	Gf′	S
ethyl malonate	S	G	G	G	G	G	R	S	S
acetone	G	SG	G	G	G	SG	S	S	S
methyl ethyl ketone	S	G	G	G	G	G	G	S	S
N,*N*-dimethylformamide	G	SG	G	G	G	SG	SG	S	S
N,*N*-dimethylacetamide	G	G	G	G	G	G	R	S	S
dimethyl sulfoxide	SG	G	G	G	G	SG	R	R	S
N-methyl-2-pyrrolidone	S	Gf	Gf	Gf	G	G	G	S	S
acetonitrile	SG	SGc	SGc	SG	SG	SG	R	R	S
methanol	SG	SGc	SGc	SG	SG	SG	R	I	I
ethanol	SG	SGc	SG	SG	SG	SG	R	R	S
1-propanol	G	SG	SG	SG	SG	SG	R	Gf	S
1-butanol	G	SG	SG	SG	SG	SG	R	Gf	S
1-octanol	G	G	G	G	G	SG	Gf′	S	S
benzyl alcohol	G	G	G	G	G	G	G	S	S
acetic acid	G	SGc	SGc	SG	SG	SG	R	S	S
hexanoic acid	S	S	S	S	S	G	G	S	S
acetic anhydride	G	SG	SG	SG	G	SG	R	R	S
propylamine	S	Gf	S	S	S	G	R	S	S
diethylamine	S	S	S	Gf′	Gf	G	G	S	S
triethylamine	S	Gf′	Gf′	Gf′	Gf′	G	SG	S	S
aniline	S	Gs	Gf′	S	Gf	G	G	Gf′	S
pyridine	S	S	S	S	Gs	G	G	S	S
triethylsilane	G	G	G	G	G	G	G	S	S
trimethylchlorosilane	S	Gf′	Gf′	Gf′	Gf′	G	R	S	S
dimethylpolysiloxane (1cs)	G	SG	SG	SG	SG	SG	R	R	R
dimethylpolysiloxane (6cs)	G	SG	SG	SG	SG	SG	R	R	R
cyclomethicone	G	SG	SG	SG	SG	SG	SG	S	S
trifluoroethanol	G	SG	SG	SGs	G	R	R	R	S
glycerol	I	I	I	I	I	I	I	I	I
water	I	I	I	I	I	I	I	I	I

[a] [Gelator] = 1–7 wt %; G = gel formed when cooled at 2–20 °C and stable at room temperature (*ca.* 20–25 °C), Gs = gel formed but turned into solution at room temperature, Gc = gel formed but turned into crystals at room temperature, SG = supergelator in which gel was formed at [gelator] < 1 wt %, Gf = gel formed when cooled in a refrigerator (at –6 °C) and stable at room temperature, Gf′ = gel formed when cooled in a refrigerator (at –6 °C) but not stable at room temperature; Gel not formed because of crystallization (R), solubilization (S), or insolubilization (I).

Provided that the primary driving force for aggregation is due to the one-dimensional stacking of the cholesterol moieties, the possible aggregation modes are illustrated as in Figure 2. When the cholesterol moieties of **2Me** have one-dimensional stacking, the azobenzene moieties can take a face-to-face orientation and the aggregation should be stabilized by the stacking of the azobenzene moieties (Figure 2a).[16] In contrast, when the cholesterol moieties of **2Me′** have one-dimensional stacking, the azobenzene moieties cannot take such a face-to-face orientation and the additional stabilization arising from the azobenzene stacking is not expected (Figure 2b).[16] This structural difference reasonably explains why **2Me** is less soluble and more aggregative than **2Me′**. This may provide a clue to explain why nature chose (*S*)-chirality for C-3 of the cholesterol skeleton.

Influence of Gelator Concentration on the Sol–Gel Phase Transition Temperature. Among cholesterol-based gelators tested

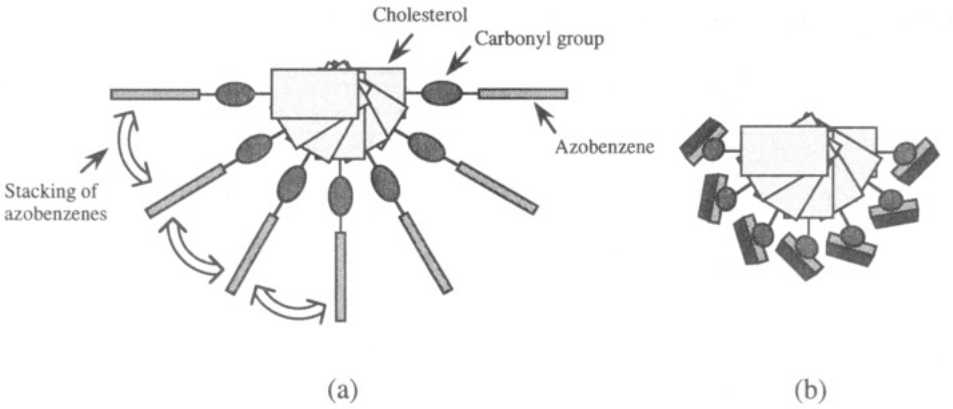

Figure 2. One-dimensional aggregation models of (a) **2Me** and (b) **2Me′**.

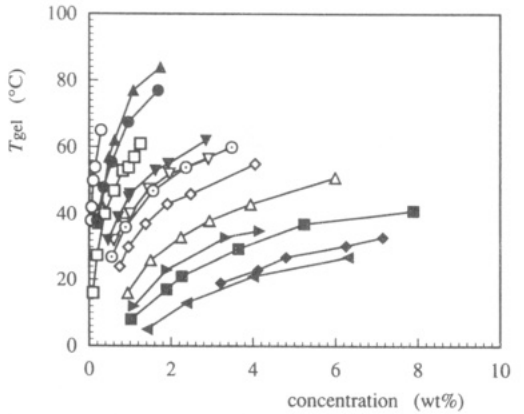

Figure 3. Plots of T_{gel} versus [**2Pr′**]: methanol (○), ethanol (□), 1-propanol (▽), 1-butanol (◇), 1-hexanol (△), 2-propanol (▼), acetone (■), *n*-hexane (◆), acetic acid (⊙), methyl acetate (◀), DMF (▶), dimethylpolysiloxane (●), and cyclomethicone (▲).

herein **2Pr′** showed the versatile gelation ability for a variety of organic solvents. This is due to the inherent nature of **2Pr′**, which has both the moderate dipole–dipole interaction for self-aggregation and the moderate affinity with solvent molecules for preventing precipitation. We thus examined the influence of the gelator concentration (mainly **2Pr′**) on the sol–gel phase transition temperature (T_{gel}). The results are shown in Figure 3 as plots of T_{gel} versus **2Pr′** concentration. The phase above each curve is the sol whereas the phase below each curve is the gel. In general, T_{gel} values rose with increasing **2Pr′** concentration and finally were saturated. In general, T_{gel} was shifted to the higher concentration region and to the lower temperature region in polar solvents. Figure 4 shows plots of the logarithm of **2Pr′** concentration vs the reciprocal absolute temperature of T_{gel}. Good linear relationships were obtained for most solvents.

Ferry et al.[17] showed a possible relationship between the concentration (C) and the gel-to-sol phase transition temperature (T_{gel}) as in eq 3 on the assumption that the formation of the

$$\ln C = -\frac{\Delta H_{fc}}{R}\frac{1}{T} + \text{constant} \qquad (3)$$

cross-link point results from a binary association of polymer chains, where ΔH_{fc} is the heat of the reaction for the concerned process and R is the gas constant. As shown later with SEM photographs, cholesterol-based gelators form fibrillar aggregates in the gel phase whereas the aggregates are dissociated into discrete

(16) The similar packing mode as illustrated in Figure 2 has been suggested by J.-H. Fuhrhop et al. (e.g., Fuhrhop, J.-H.; Demoulin, C.; Boettcher, C.; Kõnnig, J.; Siggel, U. *J. Am. Chem. Soc.* **1992**, *114*, 4159. Fuhrhop, J.-H.; Binding, U.; Siggel, U. *Ibid.* **1993**, *115*, 11036) and Y.-C. Lin in his Ph.D. Thesis (Georgetown University, 1987). In these models the size of the cross section is predicted to be one or two times the length of a single molecule. The discrepancy is probably rationalized as such that several single-molecular chains are twisted together into a strand observed by electron microscopy.

(17) Eldridge, J. E.; Ferry, J. D. *J. Phys. Chem.* **1954**, *58*, 992.

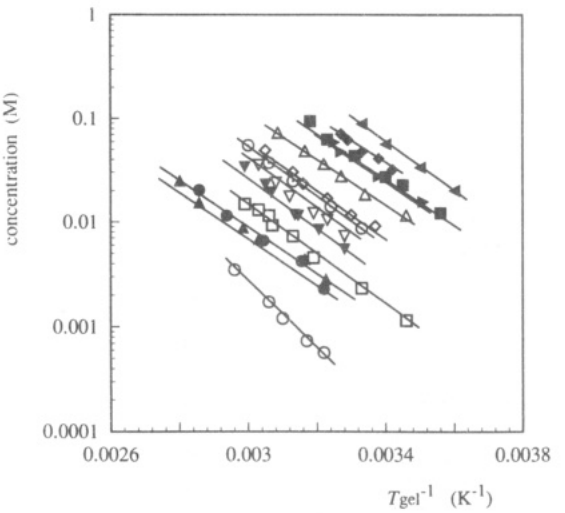

Figure 4. Plots of log [**2Pr′**] versus T_{gel}^{-1}; the symbols indicate the same solvents as those in Figure 3.

molecules in the sol phase. The gel-to-sol phase transition can then be regarded like the dissolution process of crystals. A survey of the past literatures taught us that dissolution of solid compounds into solvents is expressed by a similar equation (known as a Schrader's relation). In an ideal solution, the solubility (χ in mole fraction) at temperature T is given by eq 4,[18] where ΔH_f

$$\ln \chi = -\frac{\Delta H_f}{R}\left(\frac{1}{T} - \frac{1}{T_f}\right) \qquad (4)$$

is the melting energy and T_f is the melting point. This suggests that linear plots in Figure 4 are expressed by eq 5, which is in

$$\ln [\mathbf{2Pr'}] = -\frac{\Delta H}{R}\frac{1}{T_{gel}} + \text{constant} \qquad (5)$$

principle in the same relationship as eq 4. Clearly, both the dissolution of solid compounds into solvents and the sol-to-gel phase transition are phenomena related to disruption of intermolecular interactions followed by dispersion into homogeneous solutions. Particularly, if one could regard the **2Pr′** forming the gel network as an insoluble "solid" and the other homogeneously-dispersed **2Pr′** as "χ" (i.e., $\chi = [\mathbf{2Pr'}]_{total} - [\mathbf{2Pr'}]_{network}$), these two systems are very similar to each other. It is clear that the similarity in the physical processes is the possible reason why these two systems can be expressed by similar equations. As summarized in Table 3, ΔH values determined from the slopes in T_{gel} concentration plots in Figure 4 (ca. 45 kJ mol^{-1}) are slightly larger than ΔH_f values determined from DSC measurements at the melting point (ca. 36 kJ mol^{-1}), except for **2Dec′** gels (ΔH

(18) Moore, W. J. *Physical Chemistry*, 4th ed.; Prentice Hall Inc: Englewood Cliffs, NJ, 1972.

Table 3. ΔH Obtained from [2R] vs T_{gel} Plots[a]

gelator	solvent	T_{gel} at $C = 0.01$ M (°C)	ΔH from eq 5 (kJ mol^{-1})	ΔH_f at mp (kJ mol^{-1})
2Me′	ethanol	36	41	30
2Et′	ethanol	51	49	41
2Pr′	ethanol	53	49	36
2Bu′	ethanol	66	63	29
2Pent′	ethanol	74	65	27
2Dec′	ethanol	84	160	35
2Me′	1-butanol	7	41	30
2Et′	1-butanol	26	47	41
2Pr′	1-butanol	27	47	36
2Bu′	1-butanol	43	62	29
2Pent′	1-butanol	48	62	27
2Dec′	1-butanol	66	110	35
2Me′	1-octanol	–6	41	30
2Pr′	methanol	83	59	36
2Pr′	cyclomethicone	64	43	36
2Pr′	dimethylpolysiloxane	62	48	36
2Pr′	2-propanol	42	48	36
2Pr′	1-propanol	36	48	36
2Pr′	acetic acid	30	48	36
2Pr′	1-hexanol	16	44	36
2Pr′	DMF	7	44	36
2Pr′	acetone	5	44	36
2Pr′	*n*-hexane	–1	43	36
2Pr′	methyl acetate	–5	43	36
2Pent′	methanol	97	60	27
2Pent′	cyclomethicone	83	57	27
2Pent′	DMF	29	46	27
2Pent′	acetone	26	46	27
2Pent′	*n*-hexane	19	42	27
2Pent′	ethyl acetate	4	43	27
2Me	1-butanol	78	33	35
2Me	1-octanol	73	33	35

[a] T_{gel} at $C = 0.01$ M; in case this concentration is not included in the gel phase, the T_{gel} was obtained by extrapolation of the linear plot.

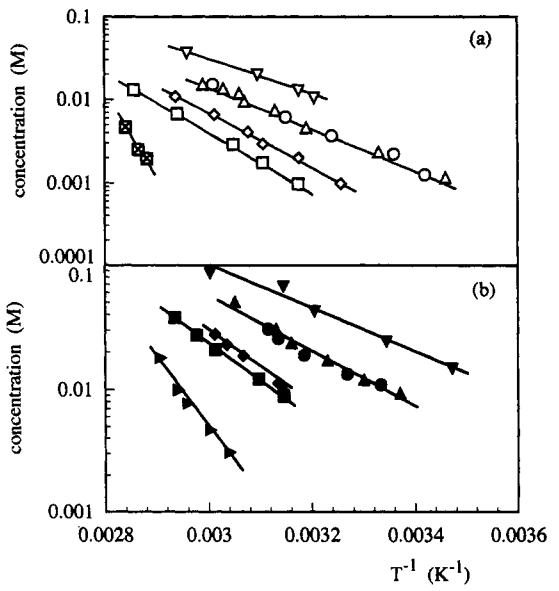

Figure 5. Plots of log [2R′] versus T_{gel}^{-1}: (a) **2Me′** in ethanol (▽), **2Et′** in ethanol (○), **2Pr′** in ethanol (△), **2Bu′** in ethanol (◇), **2Pent′** in ethanol (□), and **2Dec′** in ethanol (□); (b) **2Me′** in 1-butanol (▼), **2Et′** in 1-butanol (●), **2Pr′** in 1-butanol (▲), **2Bu′** in 1-butanol (◆), **2Pent′** in 1-butanol (■), and **2Dec′** in 1-butanol ( ).

= 110–160 kJ mol^{-1}).[19] It is also seen from Table 3 that ΔH values are scarcely affected by solvents (for example, 43–48 kJ mol^{-1} for **2Pr′** (except 59 kJ mol^{-1} in methanol)). Recently,

(19) It is not clear yet why ΔH values are larger than ΔH_f values. The most likely rationale is to consider that dissolution of the gel consists of two steps, (i) the gel-to-sol phase transition followed by (ii) discrete dispersion into the solvent, and the melting process does not include step ii.

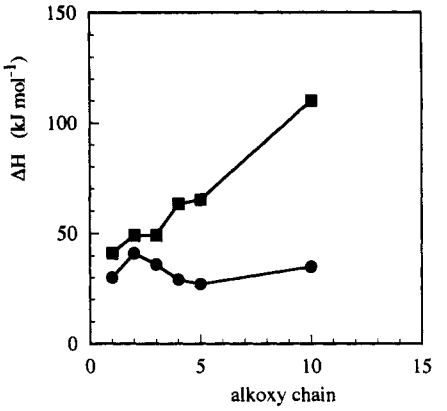

Figure 6. Plots of ΔH and ΔH_f versus the alkoxy chain of **2R′** in 1-butanol; ΔH was obtained from T_{gel} (■), and ΔH_f (melting energy) was obtained from DSC (●).

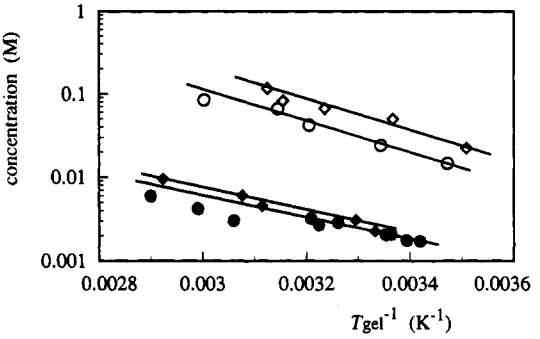

Figure 7. Plots of log [2Me] and log [2Me′] versus T_{gel}^{-1}: **2Me** in 1-butanol (●), **2Me** in 1-octanol (◆), **2Me′** in 1-butanol (○), and **2Me′** in 1-octanol (◇).

Furman and Weiss[11] investigated the gels containing cholesteryl 4-(2-anthryloxy)butanoate (CAB) and a liquid component. Their results indicated that the stability of the gelator strands depends much more upon the bulk properties of the liquid component than upon discrete CBA–solvent intermolecular interactions.[11] This implies that solvent molecules are excluded from most gelator strands and that the molecular packing of gelator strands is more or less similar to the packing of bulk crystals. These results justify the use of a Schrader's relation and reasonably explain the insensitivity to solvent effects.

Figure 5 shows the influence of R on the ΔH in ethanol and 1-butanol. It is seen from Figure 5 that the slope is affected by the length of the *p*-substituent; for example, ΔH = 41 kJ mol^{-1} for **2Me′** and 110–160 kJ mol^{-1} for **2Dec′**. Since **2R′** with the large ΔH is more soluble in ethanol or in 1-butanol, the ΔH increase is attributable to "solvation" of the R group by solvent molecules. This situation is clearly demonstrated by plots in Figure 6; that is, ΔH_f values which are not associated with solvation are almost constant whereas ΔH values which are associated with solvation of R increase with increasing R length. In Figure 7 we compare **2Me** with **2Me′** in 1-butanol and 1-octanol. When compared at the same temperature, the gelation concentration of **2Me′** is higher than that of **2Me**. This implies that **2Me′** is more soluble in these solvents. The higher affinity with solvents is reflected by the ΔH for **2Me′** (41 kJ mol^{-1}), greater by 8 kJ mol^{-1} than that for **2Me** (33 kJ mol^{-1}).

The foregoing findings are summarized as follows: (i) the ΔH is not so sensitive to the solvent effect, (ii) the *p*-substituent R is more solvated, so that the ΔH is affected by the length of R, and (iii) in general, **2R′** gives a larger ΔH than **2R** because of the higher affinity with solvent molecules.

CD Spectroscopy. Circular dichroism (CD) spectra observed for chiral molecules appear when chromophoric moieties are organized into a specific chiral orientation; for example, higher-order structures in polypeptides can provide the backbone for

Table 4. CD Spectral Parameters of **2R** and **4Cr6** Gels[a]

gelator	solvent	CD exciton type	CD $\lambda_{\theta=0}$ (nm)	CD λ_{max} (nm)	CD λ_{min} (nm)	UV λ_{max} (nm)
2Me	ethanol	positive	317	335	302	308
	1-propanol	positive	310	354	299	305
	1-butanol	positive	305	320	299	305
	1-amyl alcohol	positive	308	319	298	308
	1-octanol	positive	310	326	298	308
	2-propanol	positive	310	321	299	305
	acetone	positive	312	327	300	312
	DMF	positive	360	412	334	364
	methyl acetate	positive	331	394	310	320
	ethyl acetate	positive	310	324	300	309
	diethyl ether	positive	316	339	302	309
	n-hexane	positive	312	327	300	308
	n-heptane	positive	307	420	372	307
	methylcyclohexane	positive	308	320	299	308
2Pr	ethanol	positive	340	396	318	345
	1-propanol	positive	329	370	313	318
2Bu	ethanol	positive	342	390	323	340
4Cr6	methylcyclohexane	negative	360	333	379	358
	methylcyclohexane/benzene (9:1)	negative	353	322	408	355
	methylcyclohexane/benzene (8:2)	positive	360	403	349	358

[a] In the systems recorded in this table, the optical densities arising from LD are less than 1×10^{-3}. These values are negligibly smaller than those arising from CD.[19]

helical structures required for the appearance of the CD spectra.[20] The similar (but mechanistically-different[21,22]) CD spectra are also obtained for dye molecules in cholesteric liquid crystals[23-30] and microheterogeneously dispersed chiral molecular assemblies.[9,14,31] It occurred to us that, if the above-mentioned gelators take some specific orientation in the gel phase, the sol–gel phase transition may be conveniently detected by the CD technique.[32] As described below, we found that drastic CD changes are observed below and above the sol–gel phase transition temperature. However, it should be pointed out that orientation systems such as liquid crystals, bilayer membranes, gels, etc., are affected by macroscopic anisotropy and the observed CD spectra often include components arising from linear dichroism (LD).[22] Hence, one has to carefully discriminate the contributions of LD spectra from those of true CD spectra. We measured both CD spectra and LD spectra under the same measurement conditions. We found that in several systems the contributions of LD spectra are not negligible. We thus picked the systems in which the optical densities of the LD spectra are negligible when compared with those of the CD spectra and summarized the results in Tables 4 and 5. We can thus safely discuss the CD spectral data collected in Tables 4 and 5.

We first measured UV–visible absorption spectra above and below T_{gel}. As shown in Figure 8, the spectra for **2Me** are quite different below and above T_{gel}: the absorption maximum in the isotropic solution phase (360 nm) shifts to shorter wavelength (higher energy region) in the gel phase (310 nm).[33] This means that the excited state of the azobenzene chromophore is destabilized by molecular aggregation. Interestingly, we found that a dramatic CD spectral change takes place below and above T_{gel}. In the sol phase the solutions of **2R**, **3R**, and **4** were totally CD-silent whereas in the gel phase exciton coupling bands appeared which intersected the $\theta = 0$ line at the λ_{max} of the

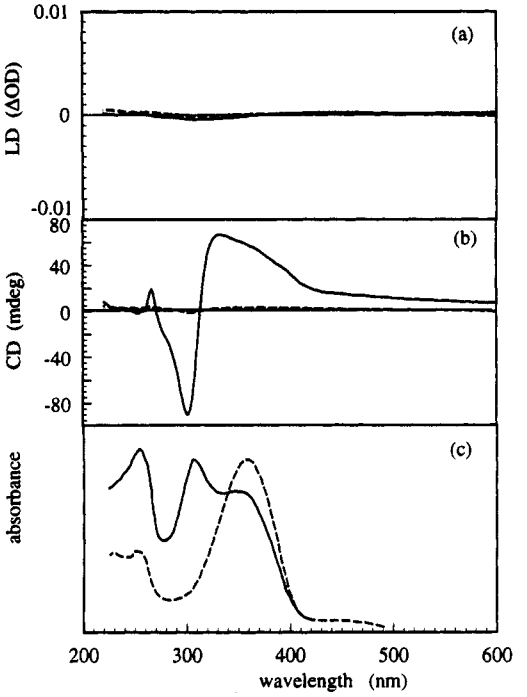

Figure 8. (a) LD spectra, (b) CD spectra, and (c) absorption spectra for **2Me** (0.2 wt %) in 1-butanol; the gel state was observed at 25 °C (—), and the solution state was observed at 60 °C (- - -).

(20) Sisido, M.; Ishikawa, Y.; Itoh, K.; Tazuke, S. *Macromolecules* **1991**, *24*, 3993.
(21) Sisido, M.; Ishikawa, Y.; Harada, M.; Itoh, K. *Macromolecules* **1991**, *24*, 3999.
(22) (a) Shindo, Y.; Nishio, M. *Biopolymers* **1990**, *30*, 25. (b) Shindo, Y.; Ohmi, Y. *J. Am. Chem. Soc.* **1985**, *107*, 91.
(23) For a comprehensive review, see: Chandrasekhar, S. In *Liquid Crystals*; Cambridge University Press: London, 1977.
(24) (a) Hatano, M. *Adv. Polym. Sci.* **1986**, *77*, 1. (b) Hatano, M.; Yoneyama, M.; Sato, Y.; Kawamura, Y. *Biopolymers* **1973**, *12*, 2423.
(25) Toriumi, H.; Yahagi, K.; Uematsu, I.; Uematsu, Y. *Mol. Cryst. Liq. Cryst.* **1983**, *94*, 267.
(26) Toriumi, H.; Uematsu, I. *Mol. Cryst. Liq. Cryst.* **1984**, *116*, 21.
(27) Sisido, M.; Kishi, R. *Macromolecules* **1991**, *24*, 4110 and reference cited therein.
(28) Kishi, R.; Sisido, M. *Makromol. Chem.* **1991**, *192*, 2723.
(29) Saeva, F. D.; Wysocki, J. J. *J. Am. Chem. Soc.* **1971**, *93*, 5928.
(30) Saeva, F. D.; Olin, G. R. *J. Am. Chem. Soc.* **1973**, *95*, 7882
(31) (a) Nakashima, N.; Fukushima, H.; Kunitake, T. *Chem. Lett.* **1981**, 1207. (b) Kunitake, T.; Nakashima, N.; Morimitsu, K. *Chem. Lett.* **1980**, 1347. (c) Nakashima, N.; Morimitsu, K.; Kunitake, T. *Bull. Chem. Soc. Jpn.* **1984**, *57*, 3253.
(32) It was shown by Lin et al.[10] and Lin in his Ph.D. Thesis (Georgetown University, 1987) that the change in the intensity of CD bands or fluorescence bands is also useful for measuring T_{gel}.

(33) In Figure 8b the exciton coupling band is not symmetrical, having an additional band at 350–450 nm. The band above 400 nm is ascribed to the n–π^* transition, but the band at around 350–400 nm which is the main source for the spectral asymmetry cannot be ascribed to the n–π^* transition. When the aggregate is disordered, the magnitude of the blue shift in the absorption maximum becomes small and it does not give an exciton coupling but a single Cotton effect. In Figure 8, in fact, the $[\theta] = 0$ wavelength in the gel phase appears at longer wavelength than the absorption maximum. Hence, the CD band at the longer wavelength region (350-400 nm) is probably due to the disorder of the aggregate. On the other hand, such a change in the absorption spectra is not observed for Figure 10; nevertheless, the CD spectrum is still asymmetrical. Probably, this is due to the overlap of an exciton coupling band with a single Cotton effect, but the reason is not clear yet.

Table 5. CD Spectral Parameters of **2R′** Gels[a]

		CD				UV
gelator	solvent	exciton type	$\lambda_{\theta=0}$ (nm)	λ_{max} (nm)	λ_{min} (nm)	λ_{max} (nm)
2Me′	methanol	positive	360	395	345	355
	ethanol	positive	372	402	346	360
2Et′	methanol	negative	357	325	415	355
	ethanol	negative	360	324	417	357
	1-propanol	positive	350	378	330	350
	1-butanol	negative	350	327	373	355
	1-amyl alcohol	negative	360	331	388	356
	2-propanol	positive	353	377	333	352
	acetone	positive	365	398	345	353
	DMF	positive	360	392	343	355
	n-hexane	negative	352	318	400	355
	cyclomethicone	negative	351	318	396	353
2Pr′	methanol	positive	360	392	340	355
	ethanol	positive	352	391	325	355
	1-butanol	positive	351	377	331	352
	1-amyl alcohol	positive	352	391	329	352
	2-propanol	positive	351	399	321	354
	cyclomethicone	negative	350	320	395	350
2Bu′	methanol	positive	360	397	345	355
	ethanol	positive	352	395	340	353
	1-propanol	negative	354	375	336	352
	1-butanol	positive	352	378	330	353
	1-amyl alcohol	positive	356	380	333	355
	2-propanol	positive	351	374	334	353
	n-hexane	negative	357	317	411	355
	cyclomethicone	negative	350	321	394	352
2Pent′	methanol	positive	356	398	342	354
	ethanol	positive	353	384	336	354
	1-propanol	negative	357	334	379	356
	1-butanol	positive	352	375	333	354
	2-propanol	positive	362	392	334	357
	DMF	positive	359	399	344	355
	ethyl acetate	positive	349	386	335	352
	n-hexane	negative	360	317	400	355
	n-heptane	negative	348	320	411	353
	methylcyclohexane	negative	363	335	418	355
	cyclomethicone	negative	348	320	411	355
2Dec′	ethanol	positive	375	411	350	365
3Me′	DMF	negative	380	365	398	385
	ethyl acetate	negative	380	365	400	385
	triethylamine	negative	380	368	397	380
	cyclohexane	negative	382	369	394	383
	methylcyclohexane	negative	383	370	395	383
	decalin	negative	383	370	396	385

[a] In the systems recorded in this table, the optical densities arising from LD are less than 1×10^{-3}. These values are negligibly smaller than those arising from CD.[19]

absorption maximum obtained in the gel phase. These findings suggest that in the gel phase cholesterol moieties in **2R**, **3R**, and **4** aggregate in a specific, chiral direction, which enforces azobenzene chromophores to interact in an asymmetric manner. Lin et al.[10] reported that anthracene-linked cholesterols give a new CD band in the gel phase, but exciton coupling bands that are useful for prediction of the direction of chirality are not observed. In Figure 9, we plotted transmittance (at 800 nm), maximum and minimum intensities of the CD spectra, and the peak ratio of 310–360 nm in the UV absorption spectra for **2Me** against the same temperature abscissa. It is clearly seen from Figure 9 that three parameters change synchronously at around 40 °C. In this gel system ([**2Me**] = 0.2 wt %), T_{gel} estimated from the mechanical test is ca. 40 °C. This supports the view that the appearance of the CD band is ascribed to the orientation of the azobenzene chromophore in the gel phase. The results indicate that the sol–gel phase transition in cholesterol-based gelators is readily "read-out" by a CD spectroscopic technique.

As shown in Figure 8, **2Me** gives a positive exciton CD spectrum which consists of the positive first Cotton effect and the negative second Cotton effect. This is a sign that two dipoles are oriented in a clockwise direction (*i.e.*, (*R*)-chirality). On the other hand, the **2Et′**–methanol gel showed a negative exciton CD spectrum which consists of the negative first Cotton effect and the positive second Cotton effect, a sign of (*S*)-chirality (Figure 10). Also, it is interesting to note that, in contrast to a significant phase-induced change in the absorption spectra of **2R**, the absorption spectra of **2R′** are scarcely changed by the phase transition. We checked the chirality of the **2R** and **2R′** gels in various solvents. The exciton types of **2R′** gels are summarized in Table 6. In general, the positive excition coupling was favored in alcohols, acetone, DMF, and ethyl acetate (*i.e.*, polar solvents) whereas the negative exciton coupling was favored in *n*-hexane, *n*-heptane, methylcyclohexane, and cyclomethicone (*i.e.*, nonpolar solvents). The results imply that the aggregate with (*R*)-chirality generates the dipole moment stronger than that with (*S*)-chirality. One can find a few exceptions in Table 6, however; for example, (i) the **2Et′** gel shows (*S*)-chirality in several alcoholic solvents (except in 1-propanol and 2-propanol) and (ii) the **2Bu′** and **2Pent′** gels show (*S*)-chirality only in 1-propanol among alcoholic solvents. The results suggest that **2Et′** as a gelator and 1-propanol as a solvent behave somewhat differently from other gelators and solvents. This reason is not understood well at present.

Unusual Inversion of CD Spectra. As recorded in Tables 4 and 5, **2Pr** and **2Bu** result in the gels with the positive exciton coupling (*i.e.*, (*R*)-chirality) and **3Me′** results in the gel with the negative exciton coupling (*i.e.*, (*S*)-chirality). Here, we accidentally found an unusual behavior about these gels: *the sign of the CD spectra is sometimes inverted!* Inversion of the CD spectra was observed for **2Pr** in ethanol and 1-propanol, **2Bu** in ethanol, and **3Me′** in

Table 6. Map of the Exciton Types of CD Spectra for 2R′ Gels[a]

gelator	2Me′	2Et′	2Pr′	2Bu′	2Pent′	2Dec′
methanol	positive	negative	positive	positive	positive	
ethanol	positive	negative	positive	positive	positive	positive
1-propanol		positive	positive	negative	negative	
1-butanol		negative	positive	positive	positive	
1-amyl alcohol		negative	positive	positive	positive	
2-propanol		positive	positive	positive	positive	
acetone		positive	positive		positive	
DMF		positive			positive	
ethyl acetate		positive			positive	
n-hexane		negative	negative	negative	negative	
n-heptane		negative			negative	
methylcyclohexane		negative			negative	
cyclomethicone (D4)		negative	negative	negative	negative	

[a] In this table, the gel systems which have CD spectral parameters sufficiently larger than the LD spectral parameters are listed (see Table 5).

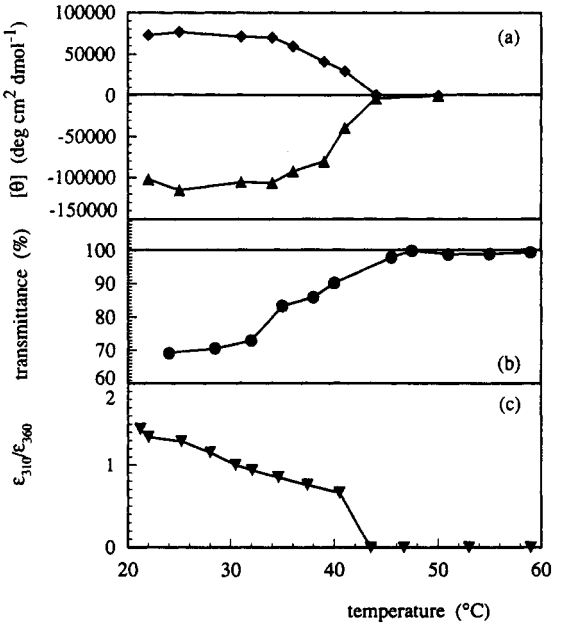

Figure 9. Temperature dependence of (a) maximum (◆) and minimum (▲) intensities of the CD spectra, (b) the transmittance at 800 nm, and (c) the ratio of the absorption spectral maxima at 310–360 nm for **2Me** (0.2 wt %) in 1-butanol.

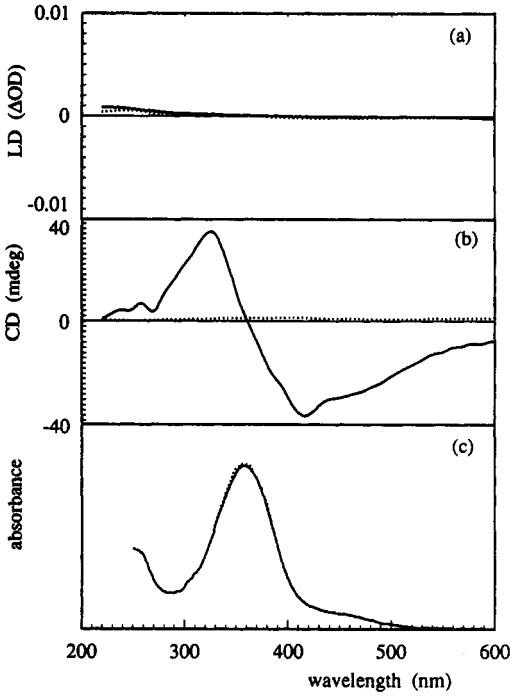

Figure 10. (a) LD spectra, (b) CD spectra, and (c) absorption spectra for **2Et′** (0.4 wt %) in methanol: the gel state at 25 °C (—) and the solution state at 65 °C (···).

cyclohexane, methylcyclohexane, and decalin.[34] We carefully examined why such inversion of the CD spectra takes place. We finally specified the reason: among several gel preparation conditions, the cooling speed is profoundly associated with the sign of the CD spectra. In Figure 11 the positive exciton coupling was obtained when the ethanol solution of **2Bu** (60 °C) was slowly cooled in air. On the other hand, the negative exciton coupling was obtained when the solution was rapidly cooled in an ice–water bath at 2 °C. Figure 12 shows the CD spectra of **3Me′** in methylcyclohexane: the cooling of the solution (60 °C) in a water bath adjusted to 30 °C gave the CD spectrum with the negative exciton coupling whereas the cooling in a water bath adjusted to 10 °C gave the CD spectrum with the positive exciton coupling. When the solution was cooled in a water bath adjusted to 25 °C, the intermediary CD spectrum was obtained. The data collected in Tables 4 and 5 are those obtained from the slow cooling method. When the **3Me′** gel with the positive exciton coupling was slowly heated, the CD sign gradually inverted from (*R*) to (*S*) (Figure 13). The critical temperature where inversion takes place is 27 °C. As mentioned above, the T_{gel} is concentration-dependent. In contrast, the critical inversion temperature was not affected by the concentration. In Figure 15 θ values for the first and second Cotton effects are plotted against temperature. When the gel with (*R*)-chirality was heated, the sign changed from (*R*) to (*S*) at 27 °C and then disappeared at the sol–gel phase transition temperature (45 °C). On the other hand, when the gel with (*S*)-chirality was cooled to −10 °C, θ values were increased to the negative direction and inversion of the sign did not take place. The results indicate that, basically, the **3Me′** gel with (*S*)-chirality is more stable than that with (*R*)-chirality. The gel with (*R*)-chirality is a metastable phase formed by the rapid cooling of the sol (the "cooling shock") and inverted to the more stable gel with (*S*)-chirality on heating. Since the θ values for the gels prepared by the gradual cooling (ca. (5–7) × 10^5) are much greater than those for the inverted gels, they should be a mixture of (*R*)- and (*S*)-chiralities, and (*S*)-chiralty exists in excess over (*R*)-chirality.

Observation of the Gel Network by a Scanning Electron Microscope (SEM). The results obtained so far consistently support the view that azobenzene-appended, cholesterol-based gelators aggregate in an asymmetric manner. In particular, the appearance of the exciton coupling bands in CD spectroscopy substantiates that these aggregates possess a helical structure. Although the gels with (*R*)- or (*S*)-chirality in the CD spectra are not necessarily twisted,[9,10] we expected that, in the present system, there may be some correlation between the strand helicity and (*R*)/(*S*)-chirality. To obtain visual insights into the aggregation mode, we prepared dry samples (see the Experimental Section) for SEM observations.

(34) Furman and Weiss[11] also found that, when mixed solvent with a critical composition is employed with CAB, two different gel types can be isolated depending upon the protocol.

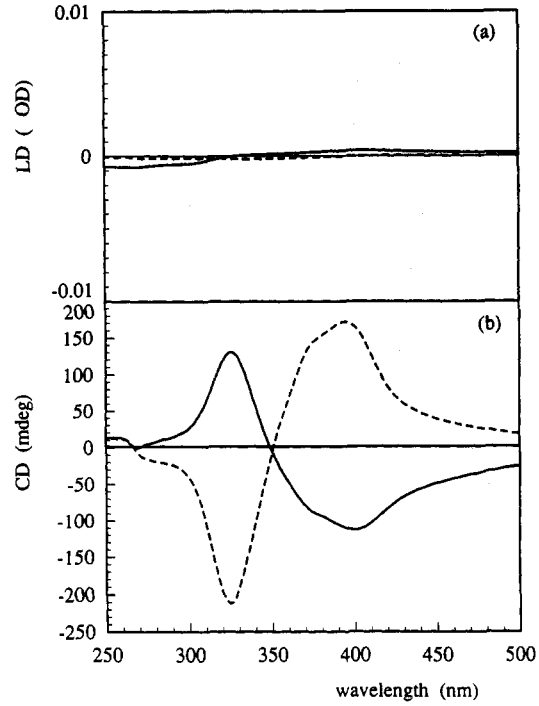

Figure 11. (a) LD spectra and (b) CD spectra of **2Bu** (0.2 wt %) in ethanol measured at 25 °C; the isotropic solution at 60 °C was cooled in ice–water at 2 °C (—), and the isotropic solution at 60 °C was held in air at 25 °C (- - -).

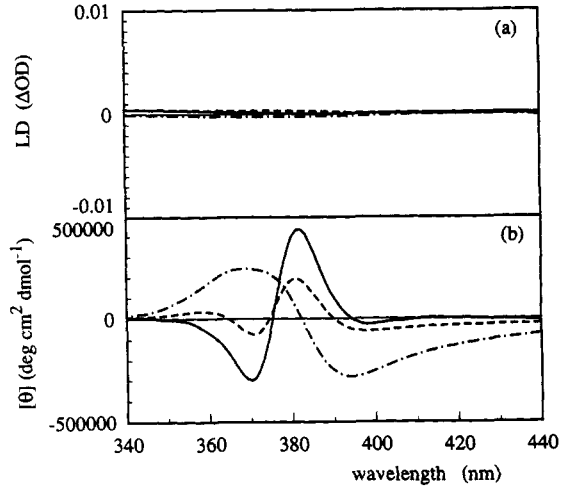

Figure 12. (a) LD spectra and (b) CD spectra of **3Me′** (0.5 wt %) in methylcyclohexane measured at 25 °C: the isotropic solution at 60 °C cooled in water at 10 °C (—), 25 °C (- - -), and 30 °C (– · –).

The gel structure obtained from the slow cooling of the **3Me′**–cyclohexane system is shown in Figure 15a. It is clearly seen from this picture that the gelator forms a three-dimensional network with 20–50-nm fibrils. We noticed, very interestingly, that *the fibrils include a left-handed helical structure!* Conceivably, **3Me′** primarily forms one-dimensional helical aggregates, which subsequently bundle up as helical fibrils. The branches are born from the knots of this helical part, suggesting that the disorder in the aggregation is the origin of the branching. Figure 15b shows a SEM picture obtained from the rapid cooling of the **3Me′**–cyclohexane system. Very interesting again, *the structure mainly consists of the right-handed helical fibrils* although the left-handed helical fibrils are partially observed as a minor structure. This is in line with our conclusions based on the CD spectral studies that the gel formed by the rapid cooling is a mixture of (*R*)- and (*S*)-chiralities.

It is now obvious that the gel with (*R*)-chirality in CD possesses the right-handed helical structure whereas the gel with (*S*)-

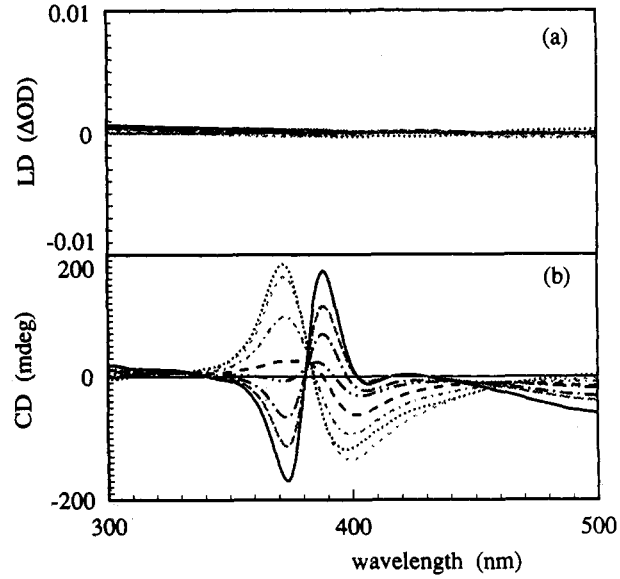

Figure 13. (a) LD spectra and (b) CD spectra for a **3Me′**-methylcyclohexane gel: 10 °C (—), 17 °C (– – –), 23 °C (– · –), 26 °C (– · · –), 28 °C (- - -), 31 °C (· · ·), 34 °C (• • •), and 37 °C (· · ·). The gel was prepared at 2 °C; [**3Me′**] = 0.5 wt %.

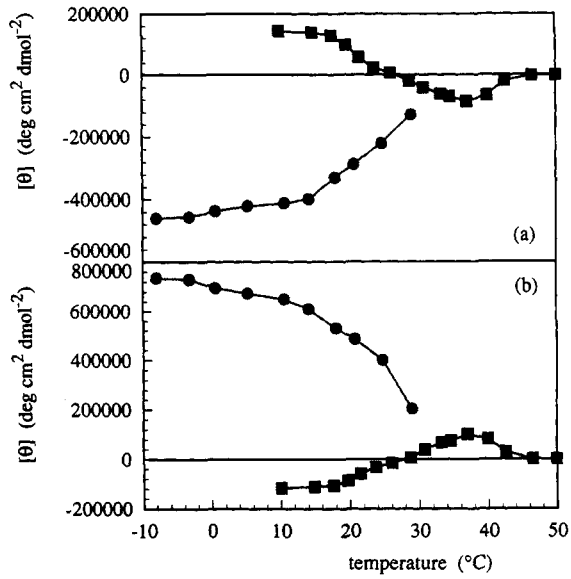

Figure 14. Temperature dependence of the intensity of (a) the first Cotton effect and (b) the second Cotton effect for **3Me′** (0.5 wt %)–methylcyclohexane gel on heating (■) and cooling (●). The gel was prepared at 2 °C.

chirality in CD possesses the left-handed structure. To give a rational explanation for inversion in the CD spectra, we have to take two possibilities into consideration. Inversion of the CD sign may be achieved by inversion of the helical structure. However, even though the helical structure is not inverted, inversion of the CD sign can take place if the cross-orientation of the azobenzene dipoles is inverted.[21] Although these two possibilities cannot be differentiated only by the CD spectral studies, the present SEM studies clearly established that inversion in CD is caused by inversion of the helical structure.

Photoinduced Sol–Gel Phase Transition. It is a most interesting property for azocholesterol derivative gel systems that the sol–gel phase transition is induced by the *trans–cis* photoisomerization of the azobenzene moiety. We prepared the **2Me** gel (0.1 wt %) in 1-butanol in 10-mm optical cell, which was photoirradiated by a 400-W high-pressure Hg lamp through a color glass filter (Toshiba UV-D35, 330 < λ < 380 nm). The spectral change was followed at 15 °C by a dual wavelength spectrophotometer. The absorption maximum at 365 nm (*trans*-**2Me**) disappeared

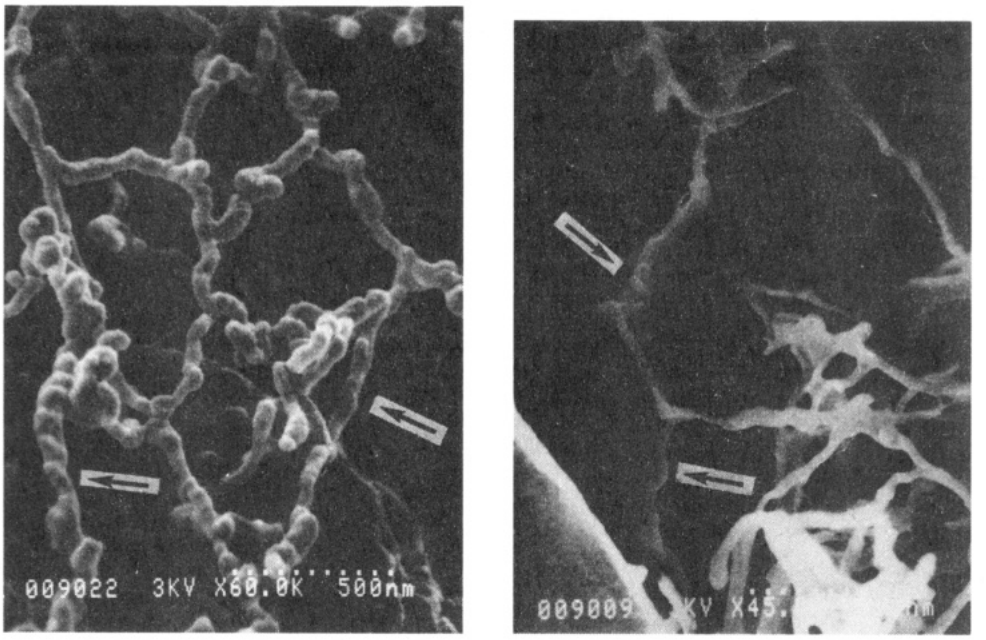

(a) (b)

Figure 15. SEM pictures of the **3Me′**–cyclohexane system: (a) slow cooling sample with a left-handed helical structure and (b) rapid cooling sample with a right-handed helical structure.

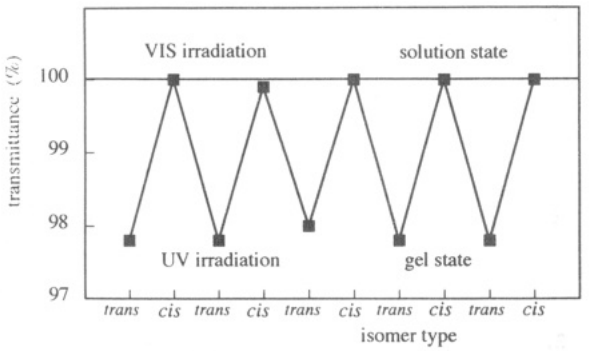

Figure 16. Photocontrol of the sol–gel phase transition for **2Me** (0.1 wt %) in 1-butanol measured at 25 °C. UV denotes irradiation of UV light ($330 < \lambda < 380$ nm), and VIS denotes irradiation of vis light ($\lambda > 460$ nm).

gradually with a tight isosbestic point at 416 nm (*cis*-**2Me**). The

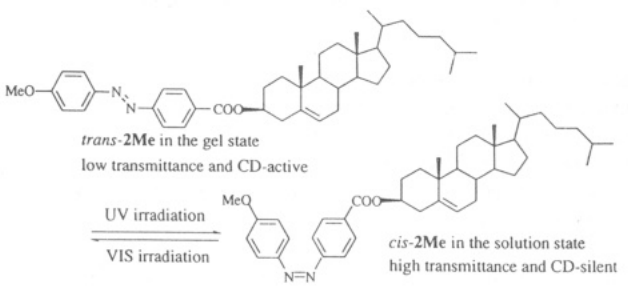

proportion of *cis* at the photostationary state was estimated to be 38%. The thermal *cis*-to-*trans* isomerization in the dark was very slow. On the other hand, *cis*-**2Me** was rapidly isomerized to *trans*-**2Me** using the same Hg lamp through a color glass filter (Toshiba Y-46, $\lambda > 460$ nm). T_{gel} was 16 °C for *trans*-**2Me** and below 2 °C for the *cis*–*trans* mixture (containing 38% *cis*-**2Me**). We thus fixed the temperature at 10 °C and photoirradiated the cell alternately by UV and vis. As shown in Figure 16, *trans*-**2Me** provided the gel with 97.8 ± 0.2% transmittance whereas the *cis*–*trans* mixture provided the sol with 100% transmittance.

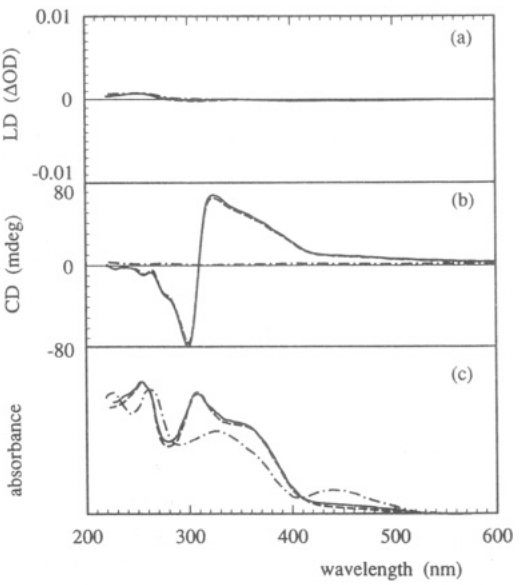

Figure 17. Photoinduced change of (a) LD spectra, (b) CD spectra, and (c) absorption spectra for **2Me** (0.2 wt %) in 1-butanol measured at 22 °C before UV irradiation (—), after UV irradiation (– • –), and after vis irradiation (– – –).

Hence, the sol–gel phase transition could be controlled reversibly by a light switch. As shown in Figure 17, the photoinduced sol–gel phase transition can be monitored by the CD technique. *trans*-**2Me** in the gel phase gave the CD spectrum with (*R*)-chirality. Upon UV irradiation the gel turned into the solution and the CD spectrum with (*R*)-chirality disappeared. Upon vis irradiation the gel was re-formed and the CD spectrum with (*R*)-chirality regenerated. Obviously, *cis*-**2Me** cannot aggregate efficiently because of the bent structure.

Experiment Section

Instrumentation. DSC was measured with a Seiko Denshi DSC-120. The heating speed was 1–3 °C min^{-1}. The formations of gels, liquid crystals, and crystals were monitored by using an optical microscope (Olympus BH-2) with a plane polarizer.

CD, LD, and UV Measurements. CD spectra and LD spectra were measured with a JASCO J-720 spectropolarimeter with a LD attachment. UV–vis absorption spectra were measured with a SHIMADZU UV-2200 spectrophotometer. A cylindrical quartz cuvette (0.1- or 0.2-mm optical path length) or a demountable flowthrough quartz cell (0.05- or 0.025-mm optical path length) was used, depending on the concentration of the gelator. The temperature was controlled by a water jacket. The gelator was mixed with the solvent in a septum-capped test tube, and the mixture was heated until the gelator was dissolved. The gel solution was put into an optical cell. The mixture was reheated by a dryer or hot water bath and cooled to form gels in an ice–water bath adjusted to ca. 2 °C (rapid cooling) or in air at ambient temperature (slow cooling). The optical densities under the measurement conditions for Tables 4 and 5 are 10^{-1}–10^{-3} for CD and less than 10^{-3} for LD. We attempted to move the samples from spot-to-spot, but the CD values were scarcely affected by rotation. Furman and Weiss[11] noticed that very thin cuvettes can influence the properties of gels when the colloidal assemblies of the gel are larger in diameter than the separation of the cuvette windows. In the present system the formation of the colloidal assemblies was not observed except for one system: only when benzene/cyclohexane mixed solvent was employed with **4Cr6**, very small colloidal assemblies appeared. The diameter estimated by SEM was 500–600 nm. Since the size is much smaller than the cuvette thickness (50 μm), the measurements were scarcely affected by the cuvette thickness.

SEM Measurements. A HITACHI S-900S scanning electron microscope was used for taking the SEM pictures. The thin gel was prepared in a 20–30-mL flask and frozen in liquid nitrogen or dry ice–methanol. The frozen specimen was evaporated by a vacuum pump for 5–24 h. The dry sample thus obtained was shielded by gold. The accelerating voltage of SEM was 3 kV, and the emission current was 10 μA.

Gelation Test in Organic Fluids. The gelator and the solvent were put in a septum-capped test tube and heated until the solid was dissolved. The solution was cooled in an ice–water bath to ca. 2 °C. When the solvent was entirely gelatinized, it was warmed to ambient temperature by air or water. If the gel existed stably, it was classified as "G" in Table 1. If the gel changed into solution, it was classified as "Gs" in Table 1. "Gc" was used when the gel gradually changed into crystals. When the solvent was not gelatinized, it was cooled in a refrigerator (at −6 °C). If the gel thus formed existed stably at room temperature, it was classified as "G_f" in Table 1. If the gel formation was observed only in the refrigerator, it was classified as "G_f'" in Table 1. "R", "S", or "I" denotes that the gel was not formed because of crystallization, solubilization, or insolubilization, respectively. Initially, the concentration of the gelator was ca. 1 wt %, and then the gelator was concentrated up to 5 wt % when the gel was not formed or dissolved in solvent.

Gel-to-Sol Transition Temperature (T_{gel}). We determined T_{gel} by three different methods: the test-tube-tilting method (method A),[35] the ball-drop method (method B),[35] and the spectroscopic turbidity method (method C). In method A, a test tube containing the gel was immersed inversely in a thermostatted water bath. In method B, a steel ball with a 3-mm diameter was put on the gel. In method C, we prepared the gel in a 10-mm optical cell and measured the transmittance at 600 nm where the cholesterol derivatives do not absorb. Here, the T_{gel} was defined as the temperature at which the gel disappears. In every case the temperature was raised at a rate of 0.2–0.3 °C min^{-1}. Three methods gave the identical T_{gel} within experimental error (±1 °C).

Semiempirical Molecular Orbital Calculations. Semiempirical molecular orbital calculations were carried out to obtain the stable structure of **2Me** and **2Me'**. Initial structures for these calculations were established using a MOLGRAPH[36] system. These molecules were fully optimized with a MOPAC93[37] program using PM3[38] Hamiltonian. Spacefilling models for each optimized structure are illustrated in Figure 1 by using a CSC Chem3D Plus[39] software. These calculations were performed on the engineering workstation system: SUN 4/10 and IRIS 4D 35G.

4-((Cholesteryloxy)carbonyl)azobenzene (1). Compound **1** was prepared according to the method in the literature:[40] yield 65%; mp 310 °C; ^{1}H NMR ($CDCl_3$) δ 0.56–2.60 (m, 43H, cholesterol), 4.50–5.20 (m, 1H, cholesterol 3-H), 5.26–5.50 (m, 1H, cholesterol 6-H), 7.16–7.58 (d, 2H, ArH), 7.75–8.23 (m, 7H, ArH); IR (Nujol) 1710 ($\nu_{C=O}$) cm^{-1}. Anal. Calcd for $C_{40}H_{54}O_2N_2$: C, 80.76; H, 9.15; N, 4.71. Found: C, 80.62; H, 9.10; N, 4.84.

4-((4-Methoxyphenyl)azo)benzoic Acid (10). To a mixture of 4-((4-hydroxyphenyl)azo)benzoic acid[41] (4.0 g, 16.6 mmol) and potassium carbonate (30.0 g, 0.16 mol) in dry DMF (100 mL) was added methyl iodide (25.0 g, 0.16 mol). The solution was allowed to stand for 16 h at reflux temperature with stirring. Compound **10** was isolated from the solution in 35% yield: mp 256–258 °C; ^{1}H NMR ($CDCl_3$) δ 3.93 (s, 3H, CH_3O), 6.90–7.38 (d, 2H, ArH), 7.80–8.40 (m, 6H, ArH); IR (Nujol) 1700 ($\nu_{C=O}$) cm^{-1}. Anal. Calcd for $C_{14}H_{12}O_3N_2$: C, 65.62; H, 4.70; N, 10.94. Found: C, 65.50; H, 4.66; N, 10.90.

4-Methoxy-4'-((cholesteryloxy)carbonyl)azobenzene (2Me). A mixture of compound **10** (1.00 g, 3.70 mmol), 4-(dimethylamino)pyridine (0.23 g, 1.90 mmol), cholesterol (1.43 g, 3.70 mmol), and dicyclohexylcarbodiimide (0.84 g, 4.07 mmol) in CH_2Cl_2 (100 mL) was stirred at room temperature for 4 h. The solvent was removed, and the product was purified by silica gel column chromatography: yield 48%; mp 302–306 °C (from DSC); ^{1}H NMR ($CDCl_3$) δ 0.30–2.65 (m, 43H, cholesterol), 3.96 (s, 3H, CH_3O), 4.70–5.26 (m, 1H, cholesterol 3-H), 5.37–5.58 (m, 1H, cholesterol 6-H), 7.00–7.46 (d, 2H, ArH), 7.85–8.42 (m, 6H, ArH); $[\alpha]_D^{25}$ 14° (*c* 0.0011, $CHCl_3$); IR (Nujol) 1710 ($\nu_{C=O}$), 1250 (ν_{C-O} methoxy) cm^{-1}. Anal. Calcd for $C_{41}H_{56}O_3N_2$: C, 78.80; H, 9.03; N, 4.48. Found: C, 78.98; H, 8.98; N, 4.55.

Related compounds (**2Et**, **2Pr**, **2Bu**, **2Dec**, **3Me**, and **3Et**) were synthesized according to a similar method.

4-Ethoxy-4'-((cholesteryloxy)carbonyl)azobenzene (2Et): yield 63%; mp 303–306 °C (from DSC); ^{1}H NMR ($CDCl_3$) δ 0.75–2.62 (m, 46H, cholesterol and CH_3), 4.02–4.28 (t, 2H, CH_2O), 4.70–5.10 (m, 1H, cholesterol 3-H), 5.30–5.56 (m, 1H, cholesterol 6-H), 6.90–7.18 (d, 2H, ArH), 7.80–8.28 (m, 6H, ArH); $[\alpha]_D^{25}$ 22° (*c* 0.0012, $CHCl_3$); IR (Nujol) 1711 ($\nu_{C=O}$), 1252 (ν_{C-O} methoxy) cm^{-1}. Anal. Calcd for $C_{42}H_{58}O_3N_2$: C, 78.95; H, 9.15; N, 4.38. Found: C, 78.84; H, 8.98; N, 4.55.

4-*n*-Propoxy-4'-((cholesteryloxy)carbonyl)azobenzene (2Pr): yield 58%; mp 293–303 °C (from DSC); ^{1}H NMR ($CDCl_3$) δ 0.58–2.62 (m, 48H, cholesterol and CH_3CH_2O), 3.91-4.18 (t, 2H, CH_2O), 4.80–5.20 (m, 1H, cholesterol 3-H), 5.50–5.60 (m, 1H, cholesterol 6-H), 6.92–7.13 (d, 2H, ArH), 7.76–8.22 (m, 6H, ArH); $[\alpha]_D^{25}$ 21° (*c* 0.0018, $CHCl_3$); IR (Nujol) 1707 ($\nu_{C=O}$) cm^{-1}. Anal. Calcd for $C_{43}H_{60}O_3N_2$: C, 79.10; H, 9.26; N, 4.29. Found: C, 79.08; H, 8.97; N, 4.19.

4-*n*-Butoxy-4'-((cholesteryloxy)carbonyl)azobenzene (2Bu): yield 52%; mp 296–302 °C (from DSC); ^{1}H NMR ($CDCl_3$) δ 0.50–2.62 (m, 50H, cholesterol and $CH_3CH_2CH_2$), 3.92–4.18 (t, 2H, CH_2O), 4.64–5.15 (m, 1H, cholesterol 3-H), 5.34–5.48 (m, 1H, cholesterol 6-H), 6.88–7.14 (d, 2H, ArH), 7.75–8.28 (m, 6H, ArH); $[\alpha]_D^{25}$ 18° (*c* 0.0013, $CHCl_3$); IR (Nujol) 1713 ($\nu_{C=O}$) cm^{-1}. Anal. Calcd for $C_{44}H_{62}O_3N_2$: C, 79.23; H, 9.37; N, 4.20. Found: C, 79.46; H, 9.32; N, 4.41.

4-*n*-Decanoxy-4'-((cholesteryloxy)carbonyl)azobenzene (2Dec): yield 45%; mp 285–292 °C (from DSC); ^{1}H NMR ($CDCl_3$) δ 0.50–2.82 (m, 62H, cholesterol and $CH_3(CH_2)_8$), 3.92–4.18 (t, 2H, CH_2O), (m, 1H, cholesterol 3-H), 5.20–5.50 (m, 1H, cholesterol 6-H), 6.88–7.14 (d, 2H, ArH), 7.80–8.30 (m, 6H, ArH); $[\alpha]_D^{25}$ 21° (*c* 0.0021, $CHCl_3$); IR (Nujol) 1711 ($\nu_{C=O}$) cm^{-1}. Anal. Calcd for $C_{44}H_{62}O_3N_2$: C, 79.95; H, 9.93; N, 3.73. Found: C, 79.67; H, 9.68; N, 4.00.

4-(Dimethylamino)-4'-((cholesteryloxy)carbonyl)azobenzene (3Me): yield 47%; mp 302–306 °C (from DSC); ^{1}H NMR ($CDCl_3$) δ 0.62–2.60 (m, 43H, cholesterol), 3.03–3.16 (s, 6H, Me_2N), 4.60–5.20 (m, 1H, cholesterol 3-H), 5.35–5.50 (m, 1H, cholesterol 6-H), 6.66–6.81 (d, 2H, ArH), 7.75–8.20 (m, 6H, ArH); $[\alpha]_D^{25}$ 55° (*c* 0.0041, $CHCl_3$); IR (Nujol) 1709 ($\nu_{C=O}$) cm^{-1}. Anal. Calcd for $C_{42}H_{59}O_2N_3$: C, 79.08 ; H, 9.32; N, 6.58. Found: C, 79.10; H, 9.40; N, 6.52.

4-(Diethylamino)-4'-((cholesteryloxy)carbonyl)azobenzene (3Et): yield 39%; mp 300 °C (from DSC); ^{1}H NMR ($CDCl_3$) δ 0.64–2.62 (m, 49H, cholesterol and CH_3), 3.28–3.60 (t, 4H, CH_2N), 4.65–5.05 (m, 1H, cholesterol 3-H), 5.29–5.48 (m, 1H, cholesterol 6-H), 6.62–6.82 (d, 2H, ArH), 7.70–8.15 (m, 6H, ArH); $[\alpha]_D^{25}$ 60° (*c* 0.0047, $CHCl_3$); IR (Nujol) 1713 ($\nu_{C=O}$) cm^{-1}. Anal. Calcd for $C_{44}H_{63}O_2N_3$: C, 79.35; H, 9.53; N, 6.31. Found: C, 79.46; H, 9.51; N, 6.25.

4-Methoxy-4'-((cholesteryloxy)carbonyl)azobenzene (2Me').[15] A mixture of compound **10** (1.69 g, 6.60 mmol), triphenylphosphine (4.57 g, 17.4 mmol), cholesterol (2.55 g, 6.59 mmol), and azenedicarboxylic acid diethyl ester (6.0 g, 34.5 mmol) in THF (100 mL) was stirred at room temperature for 24 h. The solvent was removed, and the product was purified by silica gel column chromatography: yield 55%; mp 110–

(35) Takahashi, A.; Sakai, M.; Kato, T. *Polym. J.* **1980**, *12*, 335

(36) MOLGRAPH is a molecular design support system for the IRIS workstation from DAIKIN Ind. Ltd.

(37) MOPAC93, developed by Fujitsu Ltd., Tokyo, Japan, and J. J. P. Stewart, Stewart Computational Chemistry, Copyright © FUJITSU LIMITED, 1993.

(38) Stewart, J. J. P. *J. Comput. Chem.* **1989**, *10*, 209, 221.

(39) CSC Chem3D Plus is a molecular modeling system for the Macintosh computer from Cambridge Scientific Computing, Inc.

(40) Ikeda, A.; Shinkai, S. *Rep. Asahi Glass Found. Ind. Technol.* **1992**, *61*, 115.

(41) Wallach, O.; Kiepenheuer, L. *Ber. Dtsch. Chem. Ges.* **1881**, *14*, 2617.

115 °C (from DSC); ^{1}H NMR ($CDCl_3$) δ 0.60–2.70 (m, 43H, cholesterol), 3.85 (s, 3H, CH_3O), 5.18–5.41 (m, 2H, cholesterol 3-H and 6-H), 6.90–7.18 (d, 2H, ArH), 7.78–8.18 (m, 6H, ArH); $[\alpha]_D^{25}$ −28° (*c* 0.0012, $CHCl_3$); IR (Nujol) 1711 ($\nu_{C=O}$), 1252 (ν_{C-O} methoxy) cm^{-1}. Anal. Calcd for $C_{41}H_{56}O_3N_2$: C, 78.80; H, 9.03; N, 4.48. Found: C, 78.57; H, 8.78; N, 4.63.

Related compounds (**2Et′**, **2Pr′**, **2Bu′**, **2Pent′**, **2Dec′**, **3Me′**, **3Et′**, and **3Pr′**) were synthesized according to a similar method.

4-Ethoxy-4′-((cholesteryloxy)carbonyl)azobenzene (2Et′): yield 52%; a mixture of spherulites (mp 123 °C) and needles (mp 137 °C) in a ca. 9:1 ratio; ^{1}H NMR ($CDCl_3$) δ 0.80–2.65 (m, 46H, cholesterol and CH_3), 4.01–4.31 (t, 2H, CH_2O), 5.16–5.46 (m, 2H, cholesterol 3-H and 6-H), 6.90–7.10 (d, 2H, ArH), 7.78–8.18 (m, 6H, ArH); $[\alpha]_D^{25}$ −31° (*c* 0.0014, $CHCl_3$); IR (Nujol) 1711 ($\nu_{C=O}$), 1252 (ν_{C-O} methoxy) cm^{-1}. Anal. Calcd for $C_{42}H_{58}O_3N_2$: C, 78.95; H, 9.15; N, 4.38. Found: C, 78.92; H, 9.15; N, 4.35.

4-*n*-Propoxy-4′-((cholesteryloxy)carbonyl)azobenzene (2Pr′): yield 42%; a mixture of spherulites (mp 96 °C) and needles (mp 102 °C) in a ca. 9:1 ratio; ^{1}H NMR ($CDCl_3$) δ 0.62–2.18 (m, 48H, cholesterol and CH_3CH_2O), 3.96–4.14 (t, 2H, CH_2O), 5.20–5.40 (m, 2H, cholesterol 3-H and 6-H), 6.92–7.10 (d, 2H, ArH), 7.20–8.20 (m, 6H, ArH); $[\alpha]_D^{25}$ −29° (*c* 0.0015, $CHCl_3$); IR (Nujol) 1713 ($\nu_{C=O}$), 1256 (ν_{C-O} methoxy) cm^{-1}. Anal. Calcd for $C_{43}H_{60}O_3N_2$: C, 79.10; H, 9.26; N, 4.29. Found: C, 79.14; H, 9.28; N, 4.26.

4-*n*-Butoxy-4′-((cholesteryloxy)carbonyl)azobenzene (2Bu′): yield 51%; mp 102–114 °C (from DSC); ^{1}H NMR ($CDCl_3$) δ 0.60–2.80 (m, 50H, cholesterol and $CH_3CH_2CH_2$), 3.88–4.16 (t, 2H, CH_2O), 5.15–5.37 (m, 2H, cholesterol 3-H and 6-H), 6.88–7.04 (d, 2H, ArH), 7.75–8.20 (m, 6H, ArH); $[\alpha]_D^{25}$ −19° (*c* 0.0024, $CHCl_3$); IR (Nujol) 1711 ($\nu_{C=O}$), 1255 (ν_{C-O} methoxy) cm^{-1}. Anal. Calcd for $C_{44}H_{62}O_3N_2$: C, 79.23; H, 9.37; N, 4.20. Found: C, 79.05; H, 9.29; N, 4.13.

4-*n*-Pentoxy-4′-((cholesteryloxy)carbonyl)azobenzene (2Pent′): yield 42%; mp 110–120 °C (from DSC); ^{1}H NMR ($CDCl_3$) δ 0.64–2.18 (m, 52H, cholesterol and $CH_3(CH_2)_3$), 3.96–4.18 (t, 2H, CH_2O), 5.22–5.40 (m, 2H, cholesterol 3-H and 6-H), 6.90–7.10 (d, 2H, ArH), 7.80–8.18 (m, 6H, ArH); IR (Nujol) 1711 ($\nu_{C=O}$), 1255 (ν_{C-O} methoxy) cm^{-1}. Anal. Calcd for $C_{45}H_{64}O_3N_2$: C, 79.36; H, 9.47; N, 4.11. Found: C, 79.18; H, 9.44; N, 3.94.

4-*n*-Decanoxy-4′-((cholesteryloxy)carbonyl)azobenzene (2Dec′): yield 39%; mp 123–125 °C (from DSC); ^{1}H NMR ($CDCl_3$) δ 0.50–2.82 (m, 62H, cholesterol and $CH_3(CH_2)_8$), 3.92–4.18 (t, 2H, CH_2O), 5.20–5.50 (m, 2H, cholesterol 3-H and 6-H), 6.88–7.14 (d, 2H, ArH), 7.80–8.30 (m, 6H, ArH); $[\alpha]_D^{25}$ −22° (*c* 0.0028, $CHCl_3$); IR (Nujol) 1711 ($\nu_{C=O}$) cm^{-1}. Anal. Calcd for $C_{44}H_{62}O_3N_2$: C, 79.95; H, 9.93; N, 3.73. Found. C, 80.01; H, 9.74; N, 3.55.

4-(Dimethylamino)-4′-((cholesteryloxy)carbonyl)azobenzene (3Me′): yield 38%; mp 234–238 °C (from DSC); ^{1}H NMR ($CDCl_3$) δ 0.55–2.20 (m, 43H, cholesterol), 3.07 (s, 6H, Me_2N), 5.22–5.46 (m, 2H, cholesterol 3-H and 6-H), 6.62–6.80 (d, 2H, ArH), 7.64–8.20 (m, 6H, ArH); $[\alpha]_D^{25}$ 0.5° (*c* 0.0035, $CHCl_3$); IR (Nujol) 1713 ($\nu_{C=O}$) cm^{-1}. Anal. Calcd for $C_{42}H_{59}O_2N_3$: C, 79.08; H, 9.32; N, 6.58. Found: C, 78.78; H, 9.22; N, 6.51.

4-(Diethylamino)-4′-((cholesteryloxy)carbonyl)azobenzene (3Et′): yield 32%; mp 52–58 °C; ^{1}H NMR ($CDCl_3$) δ 0.60–2.22 (m, 49H, cholesterol and CH_3), 3.32–3.60 (t, 4H, CH_2N), 5.28–5.58 (m, 2H, cholesterol 3-H and 6-H), 6.68–6.88 (d, 2H, ArH), 7.72–8.10 (m, 6H, ArH); $[\alpha]_D^{25}$ −37° (*c* 0.0046, $CHCl_3$); IR (Nujol) 1713 ($\nu_{C=O}$) cm^{-1}. Anal. Calcd for $C_{44}H_{63}O_2N_3$: C, 79.35; H, 9.53; N, 6.31. Found: C, 79.43; H, 9.46; N, 6.22.

4-(Di-*n*-propylamino)-4′-((cholesteryloxy)carbonyl)azobenzene (3Pr′): yield 28%; mp 48–58 °C (from DSC); MS (EI) 693 (M^+); ^{1}H NMR ($CDCl_3$) δ 0.64–2.62 (m, 53H, cholesterol and CH_3CH_2), 3.20–3.48 (t, 4H, CH_2N), 5.18–5.48 (m, 2H, cholesterol 3-H and 6-H), 6.60–6.80 (d, 2H, ArH), 7.78–8.20 (m, 6H, ArH); IR (Nujol) 1714 ($\nu_{C=O}$) cm^{-1}. Anal. Calcd for $C_{46}H_{67}O_2N_3$: C, 79.61; H, 9.73; N, 6.05. Found: C, 79.42; H, 9.62; N, 6.21.

In the **2R** series, the 3-H proton and the 6-H proton in the cholesterol moiety appeared separately at around 4.8 and 5.4 ppm, respectively, and the $[\alpha]_D^{25}$ values were positive (18 ~ 22°). In contrast, in the **2R′** series, the 3-H and 6-H protons appeared together at around 5.3 ppm, and the $[\alpha]_D^{25}$ values were negative (−19 ~ −31°). The differences support the view that in the **2R′** series the configuration at C-3 is inverted.

4-((4-(((Cholesteryloxy)carbonyl)methoxy)phenyl)azo)benzo-18-crown-6 (4Cr6). Thionyl chloride (0.4 g, 3.3 mmol) was added dropwise to a mixture of 4-((4-(carboxymethoxy)phenyl)azo)benzo-18-crown-6[34] (0.82 g, 1.67 mmol) and dry pyridine (0.16 g, 1.9 mmol) in dry benzene (50 mL), and the solution was refluxed for 4 h. The solvent was removed after cooling. The resultant acid chloride was dissolved in benzene (40 mL), and the solution was added dropwise to the benzene solution (10 mL) containing cholesterol (0.65 g, 1.67 mmol) and pyridine (0.16 g, 1.9 mmol). After refluxing for 9 h, the solvent was removed in vacuo. The product was isolated by silica gel column chromatography (eluent: hexane–benzene) in 63% yield: mp 130–137 °C; ^{1}H NMR ($CDCl_3$) δ 0.60–2.40 (m, 43H, cholesterol), 3.60–4.36 (m, 20H, crown), 4.50–4.84 (m, 3H, OCH_2CO and cholesterol 3-H), 5.32–5.50 (m, 1H, cholesterol 6-H), 6.60–7.14 (m, 3H, ArH), 7.40–7.96 (m, 4H, ArH); IR (Nujol) 1755 cm^{-1} ($\nu_{C=O}$). Anal. Calcd for $C_{51}H_{74}N_2O_9$: C, 71.30; H, 8.68; N, 3.26. Found: C, 71.20; H, 8.72; N, 3.13.

4-((4-(((Cholesteryloxy)carbonyl)methoxy)phenyl)azo)benzo-15-crown-5 (4Cr5). Compound **4Cr5** was synthesized from 4-((4-(carboxymethoxy)phenyl)azo)benzo-15-crown-5[34] by a similar method in 65% yield: mp 135–140 °C; ^{1}H NMR ($CDCl_3$) δ 0.58–2.40 (m, 43H, cholesterol), 3.69–4.20 (m, 16H, crown), 4.60 (s, 2H, OCH_2CO), 4.75–4.85 (m, 1H, cholesterol 3-H), 5.26–5.44 (m, 1H, cholesterol 6-H), 6.86–7.90 (m, 7H, ArH); IR (Nujol) 1750 cm^{-1} ($\nu_{C=O}$). Anal. Calcd for $C_{49}H_{70}N_2O_8$, C, 72.20; H, 8.66; N, 3.44. Found: C, 72.06; H, 8.58; N, 3.37.

Acknowledgment. We gratefully acknowledge Prof. M. Sisido for fruitful discussions on the CD spectral studies. We also acknowledge Dr. K. Nakashima, Dr. A. Ikeda, Dr. M. Takeshita, and Dr. T. James for helpful discussions and advice. We thank Prof. R. G. Weiss, who kindly sent us a copy of Lin's Ph.D. Thesis. We are indebted to Mrs. S. Uchida and Miss Y. Kawahara for measurements of NMR, IR, and MS spectra.